Optimal population transfer in combined Feshbach resonances and stimulated-Raman-adiabatic-passage processes

Phillip Price
Physics Department, University of Connecticut, Storrs, Connecticut 06269, USA

S. F. Yelin
Physics Department, University of Connecticut, Storrs, Connecticut 06269, USA
and Physics Department, Harvard University, Cambridge, Massachusetts 02138, USA

(Received 2 October 2018; revised manuscript received 23 August 2019; published 30 September 2019)

We present a method for the creation and control of cold molecules that involves coherently combining Feshbach resonances and stimulated Raman adiabatic passage. We present analytical and numerical results showing how to optimize this process that can be implemented using techniques readily available in standard experimental setups. This will provide a link in the chain from atoms to ground-state molecules and can serve as a building block towards more complex processes in coherent ultracold chemistry.

DOI: 10.1103/PhysRevA.100.033421

I. INTRODUCTION

Ultracold molecules have many potential uses in prominent areas such as quantum computation [1], control of chemical reactions [2–5], fundamental measurements [6], and few-body collision physics [1,2]. Their rich internal energy structure that makes them useful in these applications is the same property that makes these objects difficult. One standard method for creating ultracold molecules involves using resonance processes such as magnetoassociation, which makes use of a Feshbach resonance (FR) [7–11] to form vibrationally high-energy molecules from ultracold atoms. Once this process finishes, stimulated Raman adiabatic passage (STIRAP) [1,3,12,13] transfers the molecules to their ground state. One of the side effects of this methodology is that the intermediate state, vibrationally hot molecules, waits for the resonance process to end before undergoing STIRAP [14–16]. This opens the door to lose population through environmental factors, such as collisions or decay to outside states. Taking inspiration from double STIRAP procedures [2,6], we look to coherently combine the process of magnetoassociation and STIRAP in an attempt to minimize the time these molecules remain in this unstable state. By chaining these two processes together in a coherent manner we create a toolkit for true deterministic and coherent ultracold chemistry. In this paper we describe how we approach this task and the numerical optimization that goes into creating an ideal case. Ideally this technique can be used to chain together other elementary processes in this building-block-type coherent fashion.

II. MODEL DESCRIPTION

Our model describes a single coherent process from ultracold, separated atoms into ultracold molecules. Starting with separate atoms, we sweep through a Feshbach resonance to create a Feshbach molecule, i.e., a molecule in a highly excited vibrational state of the electronic ground state [14,16]. Then we apply STIRAP to the resulting molecule to transfer the molecule into a lower energy state. The key factor that makes this method useful compared to standard techniques is the coherent nature of the process. While common experimental techniques involve storing the Feshbach molecules in an optical trap and then performing STIRAP to cool them, our method is done in one continuous sweep to reduce the time the molecule spends in unstable intermediary states. Figure 1 shows a visualization of this process.

A. Model construction

Figure 2 is a visualization of the level scheme for this combined FR into STIRAP process: $|1\rangle$ represents the state of separated ultracold atoms, $|2\rangle$ represents the state of the newly combined Feshbach molecules, $|4\rangle$ represents the state of ground-state molecules, and $|3\rangle$ represents the intermediate molecular state of a standard STIRAP procedure. From this we get the following Hamiltonian for our four-level system:

$$H = \hbar \begin{bmatrix} \Delta_1 & \Omega_1 & 0 & 0 \\ \Omega_1 & \Delta_2 & \Omega_2 & 0 \\ 0 & \Omega_2 & \Delta_3 & \Omega_3 \\ 0 & 0 & \Omega_3 & 0 \end{bmatrix}. \tag{1}$$

The Δ_i are detunings of levels from their bare atomic resonances. With three transitions in the system, one of the levels ($|4\rangle$ in this case) can be set to zero (cf. Refs. [18,19]). Ω_1 is related to the width of the Feshbach resonance, while Ω_2 and Ω_3 are the pump and Stokes pulses, respectively, in a standard three-level STIRAP procedure. This model does not take into account any of the inefficiencies associated with standard magnetoassociation processes, so population numbers reflect only the percentage of Feshbach molecules that are actually created via the initial magnetic field sweep, which typically is about 20% of the ultracold atom population. We also neglect to include decay from $|3\rangle$ out of the system. As usual in

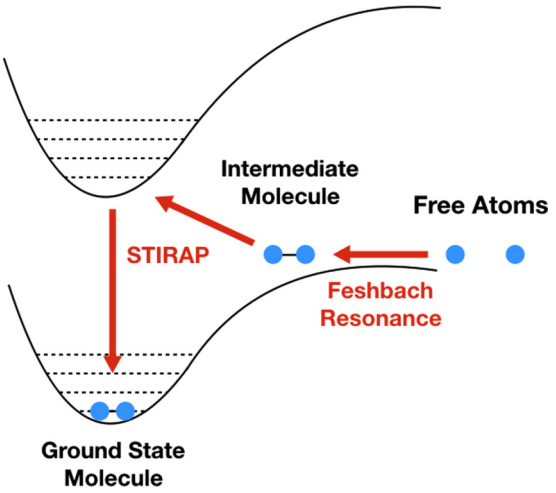

FIG. 1. General overview of the process, working from right to left. A collection of ultracold atoms goes through a Feshbach resonance to create ultracold molecules. Then, without storing these high-energy molecules, we coherently apply STIRAP to take the molecule into a more stable ground-state level. Picture inspired by Ref. [17].

STIRAP systems, the population spends negligible time in $|3\rangle$ and thus we choose to ignore additional decays from this level.

B. Feshbach resonance and rapid adiabatic passage

The major shift in framework we make is viewing the magnetoassociation process through the lens of the well-understood coherent process of rapid adiabatic passage (RAP) [4,5,20–22]. With that shift, we attempt to find a suitable dark state for this process and optimize accordingly. The energy-level anticrossings of typical (magnetic) Feshbach resonances under a changing magnetic field are analogous to the anticrossings of the dressed states of RAP, i.e., when the field is chirped. Thus the magnetic field in FR is analogous to the detuning in RAP and the strength of the FR is analogous to the coupling strength, i.e., Rabi frequency of the RAP field (see the Appendix for details). The Hamiltonian for a coupled two-channel model of FR is [9]

$$H_{tc} = \begin{bmatrix} H_{bg} & W(r) \\ W(r) & H_{cl}(B) \end{bmatrix},$$

where the diagonal elements represent the Hamiltonians of the two scattering channels in the hypothetical absence of any coupling and the off-diagonal elements represent the coupling between the two channels with r representing the distance between the atom pair. The standard Hamiltonian for RAP is

$$H_{\mathrm{RAP}} = \hbar \begin{bmatrix} 0 & \Omega \\ \Omega & \Delta(t) \end{bmatrix}.$$

According to Ref. [9] we can reduce the diagonal elements of H_{tc} to just the difference between the entrance and closed channels of the system, i.e., $H_{bg} \to 0$ and $H_{cl} \to (H_{cl}(B) - H_{bg})$. The optical detuning ($\Delta$) of a RAP process is analogous to the magnetic detuning (B) in magnetoassociation, while the Rabi frequencies (Ω) in RAP serve the same purpose as the level couplings ($W(r)$) of magnetoassociation

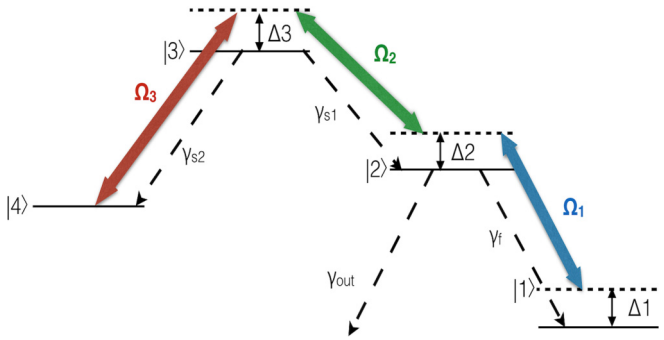

FIG. 2. Energy-level scheme for the four-level model of the system. The γ's represent the only decays we included in our calculation in the form of Lindblad operators.

in determining the width of the resonance. With RAP's dependence on Δ and magnetoassociation's dependence on a changing magnetic field B, both processes are time dependent. This analogy allows us to describe the complicated process of magnetoassociation in language similar to that used to describe STIRAP. With this translation from magnetoassociation to RAP, we can easily combine it with standard models of STIRAP and begin performing analysis on a joint FR-STIRAP system.

III. QUALITATIVE ANALYSIS

Our goal is to maximize the coherent transfer of population from $|1\rangle$ into $|4\rangle$. An easy way to do this is to find a dark state of the Hamiltonian that has components of both $|1\rangle$ and $|4\rangle$. Then we can adiabatically manipulate the parameters of our system such that the state initially is aligned along $|1\rangle$ and ends fully aligned along $|4\rangle$. This is the bare minimum we are looking for at first. Once those conditions are satisfied we would like to impose further conditions of minimizing the amount of population that is in $|2\rangle$ and $|3\rangle$ throughout the process, as those states are assumed to be the most unstable and prone to decays out of the system. The first step in finding a dark state is looking at the determinant of the Hamiltonian of Eq. (1):

$$\det H = \hbar^2\left(\Omega_1^2\Omega_3^2 - \Delta_1\Delta_2\Omega_3^2\right). \tag{2}$$

This is not identically zero, so no dark state exists *a priori* in this system. To move forward we artificially create one by enforcing certain relations between parameters, for example, by imposing the following condition:

$$\Omega_1^2 = \Delta_1\Delta_2. \tag{3}$$

With Eq. (3) the determinant of the Hamiltonian becomes zero and the following dark state appears:

$$|\Psi\rangle = \frac{1}{\Phi^2}(\Omega_1\Omega_3|1\rangle - \Delta_1\Omega_3|2\rangle + \Delta_1\Omega_2|4\rangle), \tag{4}$$

where $\Phi^2 = \sqrt{(\Omega_1\Omega_3)^2 + (\Delta_1\Omega_3)^2 + (\Delta_1\Omega_2)^2}$. As desired this dark state has components along $|1\rangle$ and $|4\rangle$. While there is an additional component along $|2\rangle$, there is no component along $|3\rangle$. Getting this dark state to initially line up with $|1\rangle$ is difficult primarily because of the dark state condition (3). Our approximation is to start with Ω_1 and Ω_2 equal to zero, with

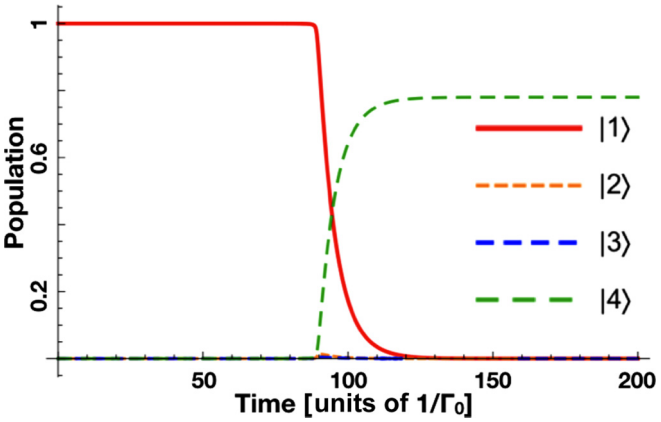

FIG. 3. A typical time evolution of the population in each of the four bare states throughout the process.

Ω_3 and Δ_2 both nonzero. Δ_3 plays no significant role in this discussion, and Δ_4 is already zero by assumption. To show this meets our criterion of initially aligning with $|1\rangle$ we solve Eq. (3) for Δ_1 and plug the result into Eq. (4):

$$|\Psi\rangle \propto \Omega_3\Delta_2|1\rangle - \Omega_1\Omega_3|2\rangle + \Omega_1\Omega_2|4\rangle.$$

With Ω_1 and Ω_2 as the small parameters, we see that $|2\rangle$ is first order in these small parameters and $|4\rangle$ is second order. Thus in the limit that these small parameters go to zero our state is initially lined up with $|1\rangle$. At the end of our process Ω_3 and Δ_2 are the small parameters, so looking at Eq. (4) we see that similarly this state ends in $|4\rangle$ with $|1\rangle$ and $|2\rangle$ both first order in the small parameters, while $|4\rangle$ is zero order.

Throughout this procedure it will be useful to look at the coupling strengths between our dark state and other states in which we wish to avoid large populations. First we move into an adiabatic basis. We choose our dark state as defined in Eq. (4) and the excited state $|3\rangle$ as two of the new basis vectors. We then use Gram-Schmidt orthogonalization to get the remaining two basis states, which will be "bright states," coupling to the excited state $|3\rangle$. The transformation matrix R

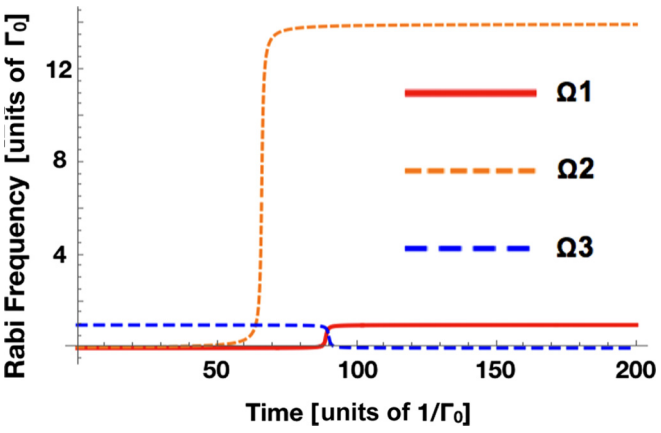

FIG. 4. Rabi frequencies (Ω's) for time evolution in Fig. 3.

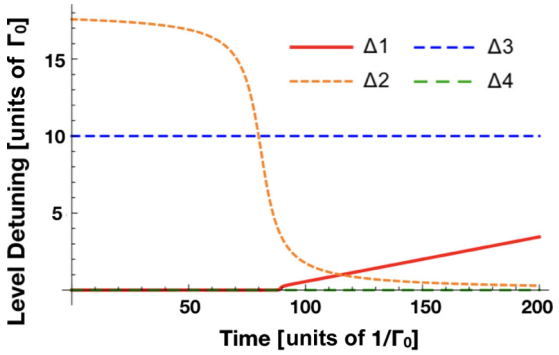

FIG. 5. Relevant level detunings for time evolution presented in Fig. 3.

then becomes

$$R = \begin{bmatrix} \frac{\Delta_1}{\Phi_1^2} & \frac{-\Delta_1\Omega_1\Omega_2}{\Phi_2^2\Phi^2} & 0 & \frac{\Omega_1\Omega_3}{\Phi^2} \\ \frac{\Omega_1}{\Phi_1^2} & \frac{\Delta_1^2\Omega_2}{\Phi_2^2\Phi^2} & 0 & \frac{-\Delta_1\Omega_3}{\Phi^2} \\ 0 & 0 & 1 & 0 \\ 0 & \frac{(\Delta_1^2+\Omega_1^2)\Omega_3}{\Phi_2^2\Phi^2} & 0 & \frac{\Delta_1\Omega_2}{\Phi^2} \end{bmatrix},$$

where columns 1 and 2 are the bright states, column 3 is the excited state, and column 4 is our dark state. For normalization, $\Phi_1^2 = \sqrt{\Delta_1^2 + \Omega_1^2}$, $\Phi_2^2 = \sqrt{\Delta_1^2\Omega_1^2\Omega_2^2 + \Delta_1^4\Omega_2^2 + \Omega_3^2(\Delta_1^2 + \Omega_1^2)^2}$, and Φ^2 is as defined previously. Since the parameters in this matrix are time dependent, the Hamiltonian transforms into

$$H' = RHR^\dagger - iR^\dagger\dot{R}. \tag{5}$$

The coupling between the dark state and the excited state is identically zero in this transformation. Therefore, in our adiabatic considerations we focus on the coupling between the dark state and the two constructed bright states. By minimizing this coupling we should be able to keep our system state closely aligned with the dark state even in the presence of incoherent processes in the system [23].

IV. NUMERICAL RESULTS

In order to give typical examples of this combined coherent process, we assume appropriate pulse forms in order to demonstrate the power of this procedure compared to traditional experimental setups. The switching on and off of the field can be described in terms of an arctangent function:

$$\Omega_i(t) = \frac{\Omega_{\text{mag}}}{\pi}\left(\frac{\pi}{2} \pm \arctan\left(\frac{t - t_0}{\tau}\right)\right),$$

where Ω_{mag}, t_0, and τ are the numerical parameters that form the search space. The form is such that for $-$ (+) the Ω's start (end) at zero and end (start) at Ω_{mag}. We also take a similar form for Δ_2, where Δ_2 starts near its maximal value and ends near zero. Δ_1 is numerically determined by the dark state condition (3).

For simplicity we define a decay rate Γ_0 which we use to set the units for all our relevant parameters. Setting the decay rates $\gamma_f = \gamma_{\text{out}} = 2\Gamma_0$ and $\gamma_{s1} = \gamma_{s2} = 20\Gamma_0$, we found a typical evolution, represented by Fig. 3.

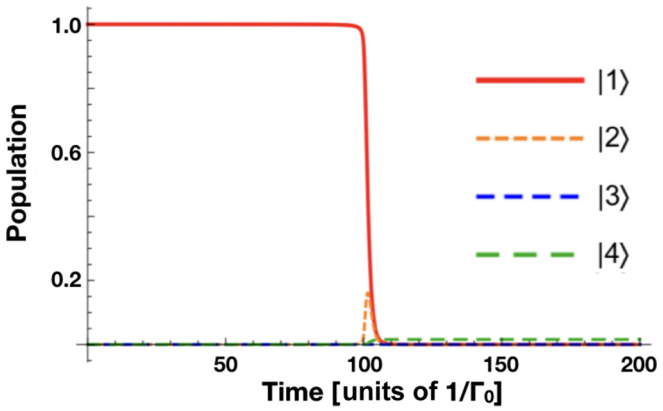

FIG. 6. Time evolution of populations with FR and STIRAP as separate processes when the decay of state $|2\rangle$ is not vanishingly small ($2\Gamma_0$). This was optimized in a similar way as Fig. 3, using the same decay rates but varying the strength and time scale of the Rabi frequencies and level detunings.

Figures 4 and 5 show the Rabi frequencies and detunings, respectively, needed to achieve this result. Note that the decay rates are near the magnitude of the Rabi frequencies needed to achieve this result.

This is a considerably better result than what can be achieved by treating the same four-level system as two separate coherent processes of RAP followed by STIRAP, as seen in Fig. 6. This is a massive improvement for a medium-strength decay out of the system. While very strong decay out of the system will, up to now, produce similar results, this alternative method shows much improvement over treating these two processes independently. Note that with more unfavorable decay rates and Rabi frequencies than presented in Ref. [16] our calculations yield similar or better results.

Results for different combinations of system parameters (in particular, different strengths of decay out of state $|2\rangle$) are shown in the Appendix.

V. CONCLUSION

This work provides an alternative and easily testable framework for the creation of ultracold molecules. In addition, this coherent combination of the two steps can, in principle, be inserted anywhere needed in a chain of steps, joining together any resonant and STIRAP processes. Current experimental setups should be able to incorporate these ideas fairly easily, as the proposed method does not call for new equipment, merely an adjustment of standard techniques by adjusting to time-dependent Rabi frequencies and detunings. One issue this work does not address yet is the relative inefficiency of the resonant process, in our case the Feshbach resonance. Due to the coherent nature of the STIRAP procedure, any combination of Feshbach resonance and STIRAP can only be used once, since repeated applications would empty the final state at the same rate as it would be filled. Further study into multiple iterations of this pulse scheme could mitigate that particular issue, altering this method to facilitate multiple runs that will capture more ground-state molecules than are destroyed. This will be subject of an upcoming publication. Further improvement on the method presented here could be achieved by taking advantage of the strong coupling between the intermediate levels $|2\rangle$ and $|3\rangle$ [24].

ACKNOWLEDGMENTS

We would like to thank Robin Côtè and Florentin Reiter for helpful discussions. We would also like to acknowledge funding from the National Science Foundation.

APPENDIX

Here we give the entries from the transformed matrix H' mentioned in Eq. (5):

$$
\begin{aligned}
H'_{11} &= \Delta_1 + \frac{\Omega_1^2}{\Delta_1},\\
H'_{22} &= 0,\\
H'_{33} &= \Delta_3,\\
H'_{44} &= 0,\\
H'_{12} &= \frac{i\Delta_1\Omega_2(\Delta_1\dot{\Omega}_1 - \dot{\Delta}_1\Omega_1)}{\sqrt{\Delta_1^2+\Omega_1^2}\sqrt{(\Delta_1^2+\Omega_1^2)(\Omega_1^2\Omega_3^2+\Delta_1^2(\Omega_2^2+\Omega_3^2))}},\\
H'_{13} &= \frac{\Omega_1\Omega_2}{\sqrt{\Omega_1^2+\Omega_2^2}},\\
H'_{14} &= \frac{i\Omega_3(\Omega_1\dot{\Delta}_1 - \Delta_1\dot{\Omega}_1)}{\sqrt{\Delta_1^2+\Omega_1^2}\sqrt{\Omega_1^2\Omega_3^2+\Delta_1^2(\Omega_2^2+\Omega_3^2)}},\\
H'_{23} &= \frac{\sqrt{(\Delta_1^2+\Omega_2^2)(\Omega_1^2\Omega_3^2+\Delta_1^2(\Omega_2^2+\Omega_3^2))}}{\Delta_1^2+\Omega_1^2},\\
H'_{24} &= \frac{i(\Delta_1\Omega_1\Omega_2\Omega_3\dot{\Omega}_1 + \Delta_1^3(\Omega_2\dot{\Omega}_3 - \dot{\Omega}_2\Omega_3) - \Omega_1^2(\Delta_1\Omega_3\dot{\Omega}_2 + \Omega_2(\Omega_3\dot{\Delta}_1 - \dot{\Omega}_3\Delta_1)))}{\sqrt{\Omega_1^2\Omega_3^2+\Delta_1^2(\Omega_2^2+\Omega_3^2)}\sqrt{(\Delta_1^2+\Omega_1^2)(\Omega_1^2\Omega_3^2+\Delta_1^2(\Omega_2^2+\Omega_3^2))}},\\
H'_{34} &= 0.
\end{aligned}
$$

TABLE I. Explicit parameter values.

	Parameters	Fig. 3	Fig. 7	Fig. 8
$\Omega 1$	$\Omega 1_{\text{mag}}[\Gamma_0]$	1	1	1
	$\Omega 1_{\text{offset}}[\Gamma_0^{-1}]$	89	89	89
	$\Omega 1_{\tau}[\Gamma_0^{-1}]$	0.5	0.5	0.5
$\Omega 2$	$\Omega 2_{\text{mag}}[\Gamma_0]$	14	14	14
	$\Omega 2_{\text{offset}}[\Gamma_0^{-1}]$	66	66	66
	$\Omega 2_{\tau}[\Gamma_0^{-1}]$	0.5	0.5	0.5
$\Omega 3$	$\Omega 3_{\text{mag}}[\Gamma_0]$	1	1	0.5
	$\Omega 3_{\text{offset}}[\Gamma_0^{-1}]$	90	90	90
	$\Omega 3_{\tau}[\Gamma_0^{-1}]$	0.5	0.5	0.5
$\Delta 2$	$\Delta 2_{\text{mag}}[\Gamma_0]$	18	18	18
	$\Delta 2_{\text{offset}}[\Gamma_0^{-1}]$	81	81	81
	$\Delta 2_{\tau}[\Gamma_0^{-1}]$	6	6	6
$\Delta 3$	$\Delta 3_{\text{mag}}[\Gamma_0]$	10	10	10
	$\Delta 3_{\text{offset}}[\Gamma_0^{-1}]$	0	0	0
	$\Delta 3_{\tau}[\Gamma_0^{-1}]$	0	0	0
	$\gamma_f[\Gamma_0]$	2	2	2
	$\gamma_{S1}[\Gamma_0]$	20	20	20
	$\gamma_{S2}[\Gamma_0]$	20	20	20
	$\gamma_{\text{out}}[\Gamma_0]$	2	0.2	20

We also list here the explicit parameter values (Table I) and give results for different combinations of system parameters in Figs. 7, 8, and 9. One thing of note from Fig. 9 is how robust this procedure is with regards to the decay from $|2\rangle$ into $|1\rangle$. The only thing that changes from Fig. 3 is removing the decay from $|2\rangle$ to outside of the system, yet the improvement in performance is quite noticeable.

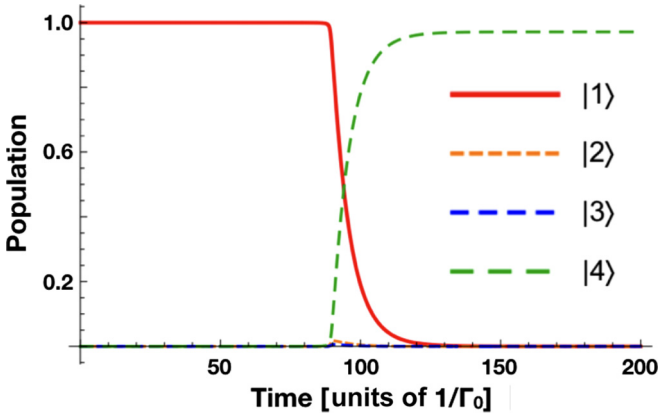

FIG. 7. Populations in the levels with γ_f and γ_{out} an order of magnitude smaller than the figures presented in the main body of the paper.

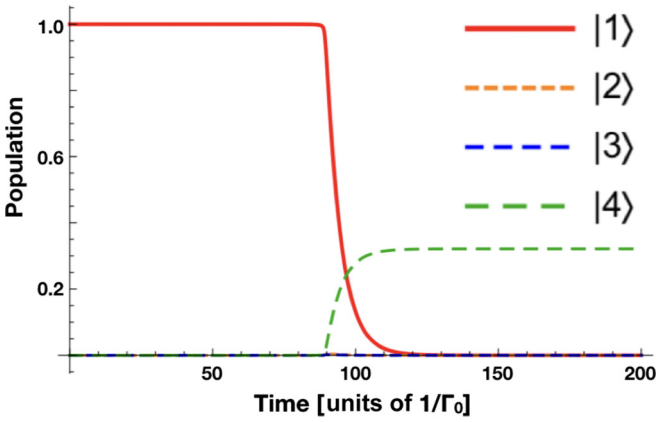

FIG. 8. Populations in the levels with γ_f and γ_{out} an order of magnitude larger than the figures presented in the main body of the paper.

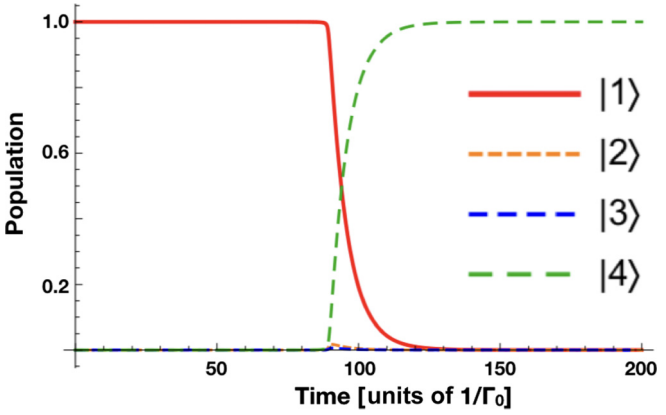

FIG. 9. This is a similar run to what is presented in Fig. 3 but with γ_{out} set to zero.

Finally, we also include RAP and Feshbach resonance energy structure in Fig. 10.

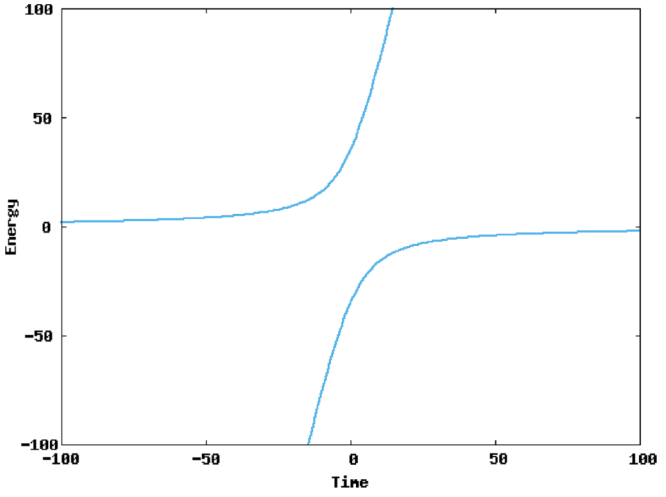

FIG. 10. Plot of the energy eigenvalues of a two-level RAP system. These are similar in structure to what is presented in Fig. 13 in Ref. [11]. Treating the magnetic field as a function of time, we can translate from magnetic field on the x axis [11] to time on the x axis, as we have plotted here.

[1] K. Winkler, F. Lang, G. Thalhammer, P. v. d. Straten, R. Grimm, and J. H. Denschlag, Phys. Rev. Lett. **98**, 043201 (2007).
[2] J. G. Danzl, E. Haller, M. Gustavsson, M. J. Mark, R. Hart, N. Bouloufa, O. Dulieu, H. Ritsch, and H.-C. Nägerl, Science **321**, 1062 (2008).
[3] N. Vitanov, M. Fleischhauer, B. Shore, and K. Bergmann, Adv. At. Mol. Opt. Phys. **46**, 55 (2001).
[4] N. V. Vitanov, T. Halfmann, B. W. Shore, and K. Bergmann, Annu. Rev. Phys. Chem. **52**, 763 (2001).
[5] V. S. Malinovsky and J. L. Krause, Eur. Phys. J. D **14**, 147 (2001).
[6] E. Kuznetsova, P. Pellegrini, R. Côté, M. D. Lukin, and S. F. Yelin, Phys. Rev. A **78**, 021402(R) (2008).
[7] E. Tiesinga, B. J. Verhaar, and H. T. C. Stoof, Phys. Rev. A **47**, 4114 (1993).
[8] P. Courteille, R. S. Freeland, D. J. Heinzen, F. A. van Abeelen, and B. J. Verhaar, Phys. Rev. Lett. **81**, 69 (1998).
[9] T. Köhler, K. Góral, and P. S. Julienne, Rev. Mod. Phys. **78**, 1311 (2006).
[10] P. S. Julienne, E. Tiesinga, and T. Köhler, J. Mod. Opt. **51**, 1787 (2004).
[11] C. Chin, R. Grimm, P. Julienne, and E. Tiesinga, Rev. Mod. Phys. **82**, 1225 (2010).
[12] E. A. Shapiro, M. Shapiro, A. Pe'er, and J. Ye, Phys. Rev. A **75**, 013405 (2007).
[13] K. Bergmann, H. Theuer, and B. W. Shore, Rev. Mod. Phys. **70**, 1003 (1998).
[14] K.-K. Ni, S. Ospelkaus, M. H. G. de Miranda, A. Pe'er, B. Neyenhuis, J. J. Zirbel, S. Kotochigova, P. S. Julienne, D. S. Jin, and J. Ye, Science **322**, 231 (2008).
[15] J. G. Danzl, M. J. Mark, E. Haller, M. Gustavsson, R. Hart, J. Aldegunde, J. M. Hutson, and H.-C. Nägerl, Nat. Phys. **6**, 265 (2010).
[16] S. Ospelkaus, A. Pe'er, K.-K. Ni, J. J. Zirbel, B. Neyenhuis, S. Kotochigova, P. S. Julienne, J. Ye, and D. S. Jin, Nat. Phys. **4**, 622 (2008).
[17] S. Cornish, Physics **1**, 24 (2008).
[18] J. Oreg, K. Bergmann, B. W. Shore, and S. Rosenwaks, Phys. Rev. A **45**, 4888 (1992).
[19] Y. B. Band and P. S. Julienne, J. Chem. Phys. **95**, 5681 (1991).
[20] D. Grischkowsky and M. M. T. Loy, Phys. Rev. A **12**, 1117 (1975).
[21] M. M. T. Loy, Phys. Rev. Lett. **32**, 814 (1974).
[22] D. Grischkowsky, Phys. Rev. A **14**, 802 (1976).
[23] Q.-C. Wu, Y.-H. Chen, B.-H. Huang, J. Song, Y. Xia, and S.-B. Zheng, Opt. Express **24**, 22847 (2016).
[24] F. Reiter and A. S. Sørensen, Phys. Rev. A **85**, 032111 (2012).